

ELECTROMAGNETIC INTERACTION OF A SMALL MAGNET AND A WALL-BOUNDED FLOW WITH CONDUCTING WALLS

KAZAK¹ O., HEINICKE^{1,2} CH., WONDRAK³ T., BOECK¹ T.

¹ Institute of Thermodynamics and Fluid Mechanics, Ilmenau University of Technology, P.O. Box 100565, 98684 Ilmenau, Germany

² Department of Applied Mechanics, Aalto University, PO Box 14300, 00076 Aalto, Finland

³ Helmholtz-Zentrum Dresden-Rossendorf, Bautzner Landstraße 400, 01328 Dresden, Germany

E-mail address of corresponding author: oleg.kazak@tu-ilmenau.de

Abstract: We study the effects of electrically conducting walls on the interaction between a small cubic permanent magnet and liquid-metal flow in a cylindrical pipe using experiments and electromagnetic simulation. The problem is motivated by Lorentz force velocimetry, where the drag force on the magnet due to the induced eddy currents in the flow is used for flow measurement. Compared with insulating walls, the conducting walls lead to an increased drag force on the magnet. Except for low distances, the experimental results are satisfactorily reproduced in simulations using a point dipole approximation of the magnetic field.

1. Introduction

In recent years several novel methods for flow measurement based on electromagnetic induction have been developed. They work without direct contact with the molten metal, whereby the problems due to high temperature and chemical aggressiveness of these materials can be circumvented. One of them is the so-called Lorentz force velocimetry (LFV) [1]. In this method, a magnet next to the moving conducting fluid causes induction of eddy currents, which give rise to a braking Lorentz force on the flow. An equal but opposite force acts on the magnet, which can be measured. It depends on the magnitude and distribution of velocity and magnetic field in the flow domain. Several studies of LFV have examined the influence of the distance between magnet and fluid as well as effects of field distribution [2, 3]. We extend these previous studies by examining the influence of finite conducting walls between the magnet and conducting liquid.

2. Presentation of the problem

Local flow measurement with LFV can be realized when the magnetic field is only significant in a limited flow volume. For such purposes one can use small permanent magnets. First investigations in this direction were performed on duct flows with insulating walls [2]. The same equipment, i.e. magnet and force sensor, were also used in the present study. Lorentz force measurements were taken for flows of the alloy InGaSn in cylindrical pipes with insulating and conducting walls. The setup was the same as in previous studies of other flow sensors for conducting flows [4]. The walls of the three pipes are made from copper, brass and PVC. The flows are driven by an electromagnetic pump and the mean flow velocity is controlled by an inductive flow meter (ABB Copa-XL DN25). In the experimental study, the position of the cubic permanent magnet relative to the pipe was changed systematically in the radial and transverse directions, and the flow velocity was varied. For one measurement the drag component of the Lorentz force was recorded with a temporal resolution of 6.4 Hz and averaged over 40 s.

Differences between insulating and conducting pipe walls originate from different eddy current distributions. Although there is no induction in the stationary walls, the eddy currents generated in the liquid will pass through the conducting walls, and can thereby change the resulting Lorentz force.

For the numerical simulation of the problem we use the geometry and coordinate system shown in Fig. 1. The central axis of the pipe coincides with the x-axis. We only consider a finite section of the pipe in the axial direction whose length is adjusted depending on the distance of the magnet to the pipe.

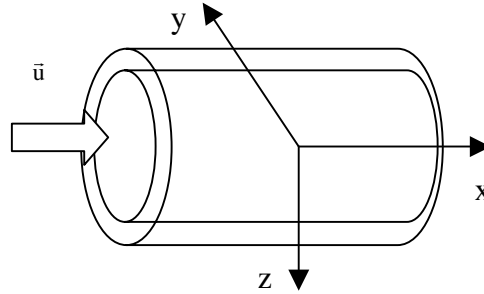


Figure 1: Pipe with conducting walls and coordinate system.

The geometrical and material properties are as follows: inner pipe diameter $d_1 = 27 \cdot 10^{-3}$ m, thickness of the wall $d_2 = 2.7 \cdot 10^{-3}$ m, wall conductivity for copper $\sigma_1 = 58 \cdot 10^6$ S/m, conductivity of InGaSn $\sigma_2 = 3.3 \cdot 10^6$ S/m, kinematic viscosity of InGaSn $\nu = 3.4 \cdot 10^{-7}$ m²/s, density of InGaSn $\rho = 6492$ kg/m³.

With these parameters one can estimate the Reynolds and magnetic Reynolds numbers for an average velocity $u = 1$ m/s that we consider in the simulations. The Reynolds number is $Re = ud_1/\nu = 8 \cdot 10^4$, i.e. the flow is fully turbulent. The magnetic Reynolds number $Re_m = \mu_0 \sigma_2 u d_1 \approx 10^{-2} \ll 1$ is low in this problem. We therefore use the quasistatic limit of the induction equation. We also assume the velocity field to be unaffected by the Lorentz force because the values are fairly small. The mean turbulent velocity distribution in the pipe is represented by [6]

$$u_x(\mathbf{r}) = \frac{u_\tau}{\kappa} \ln \left(1 + \kappa \frac{u_\tau R}{\nu} \frac{1}{2} \left(1 - \frac{r^2}{R^2} \right) \right); \quad (1)$$

where u_τ is the friction velocity, $\kappa = 0.42$ is the von Karman constant, and $R = d_1/2$ is the inner pipe radius. The friction velocity is obtained by the constraint that (1) has to provide the correct value of the known mean velocity u . For $u=1$ m/s we obtain $u_\tau = 0.074$ m/s.

In the quasistatic formulation of the induction equation the induced currents are given by Ohm's law with the induced electric field represented by the negative electric potential gradient. Charge conservation then provides [5]

$$\nabla^2 \phi = \nabla \cdot (\bar{\mathbf{u}} \times \bar{\mathbf{B}}) \quad (2)$$

in the liquid. In the solid wall the velocity is absent, therefore

$$\nabla^2 \phi = 0. \quad (3)$$

The magnetic field is represented as a magnetic point dipole with magnetic moment $\vec{\mathbf{m}}$. When the dipole is at the origin of the coordinate system, the field distribution is [1]

$$\vec{\mathbf{B}}(\vec{\mathbf{r}}) = \frac{\mu_0}{4\pi} \left(3 \frac{\vec{\mathbf{m}} \cdot \vec{\mathbf{r}}}{r^5} \vec{\mathbf{r}} - \frac{\vec{\mathbf{m}}}{r^3} \right). \quad (4)$$

The eddy current density in the conducting walls is represented by

$$\vec{j}_1 = -\sigma_1 \nabla \phi_1 \quad (5)$$

and the eddy currents in the liquid by

$$\vec{j}_2 = \sigma_2 (-\nabla \phi_2 + \vec{u} \times \vec{B}). \quad (6)$$

The Lorentz force density is given by

$$\vec{F}_L = \vec{j} \times \vec{B}. \quad (7)$$

The boundary conditions (cf. fig. 1) are as follows:

- at the distance $R = 13.5 \cdot 10^{-3}$ m (inner pipe radius) from the x-axis the continuity boundary condition is

$$\vec{n} \cdot (\nabla \phi_1 - \nabla \phi_2) = 0; \quad (8)$$

- at the distance $R + d_2 = 16.2 \cdot 10^{-3}$ m from the x-axis the insulating boundary condition is

$$\vec{n} \cdot \nabla \phi = 0, \quad (9)$$

where \vec{n} denotes the normal vector.

The magnetic fields in the experimental setup are generated by a cubic permanent magnet with a side length of $l=10$ mm, which is approximated by a magnetic point dipole located at the centre of the permanent magnet in the numerical simulations. The magnetic moment \vec{m} in this case can be calculated from the measured distribution [2] of the magnetic field \vec{B} at larger distances according to Eq. (4). The numerical value is $m = 1.1 \text{ A}\cdot\text{m}^2$.

For the numerical solution of the Poisson equations (2, 3) for the electric potential the PDE module in the Comsol 4.4 software package was taken. Different non-uniform meshes were tested. The domain area was split into elements unevenly: in the area near the permanent magnet, where large gradients of the magnetic field are situated, the elements were of small size. Mesh convergence tests were also carried out to ensure valid results. Typical numbers of elements were about 10^6 .

3. Results

Figs. 2 and 3 show a comparison of experimental data and computational results for the total Lorentz force (obtained by integrating Eq. (7) over the whole conducting volume) at different positions of the permanent magnet for a copper pipe and an insulating PVC pipe. The magnetic moment of the cubic permanent magnet is perpendicular to the top and bottom sides of the magnet. In Figs. 2 and 3 the magnetic moment is always aligned with the z-axis. In Fig. 2 the center of the magnet is located on the z-axis (for $a=0$) and the bottom side of the magnet touches the wall of the pipe. From this reference configuration the magnet is then shifted by a distance a in the transverse direction, i.e. a is the y-position of the center of the magnet. In Fig. 3 the reference configuration ($b=0$) is the same, i.e. the center of the magnet is located on the z-axis and the bottom side of the magnet touches the pipe wall. The magnet is then shifted radially along the z-axis, and b denotes the displacement (in z) of the magnet from the reference configuration.

In both Fig. 2 and Fig. 3 the conducting walls consistently provide a higher Lorentz force, which decreases rapidly with the distance. The theoretical values from the computations overestimate the measured values. The disagreement between theory and experiment is significant at small distances and decreases with increase of a and b . This is not surprising since the dipole representation significantly overestimates the magnetic field at distances of the order of the side length of the magnet.

The relative error between experiment and theory is further illustrated in Fig. 4, which shows the ratio between theoretical and experimental Lorentz force values as function of distance. For both displacements (a and b) the error is as large as 80% at close distances and drops to about 2% or less at the largest distances. For the insulating pipe good agreement is

found at smaller distances than for the copper pipe. This observation can be attributed to the effectively larger distance between eddy currents and field source for insulating walls, which implies that the dipole approximation of the field is more accurate. The same argument also suggests that – irrespective of the distance – forces are larger for conducting walls. We also remark that the non-monotonous behaviour with respect to b in Fig. 4 is not visible in Fig. 3. It could be due to measurement errors but we cannot completely rule out mesh effects.

Fig. 5 shows distributions of eddy current and Lorentz force densities on the inner surface of the pipe. The current density and Lorentz force are given in non-dimensional form

$$\text{as } \mathbf{j}_0 = \frac{\mathbf{j}}{j_{\text{scale}}}, \quad \text{where } j_{\text{scale}} = \frac{\sigma_2 \mathbf{u} \mu_0 \mathbf{m}}{4\pi r^3} \quad \text{and} \quad F_{L0} = \frac{F_L}{F_{L\text{scale}}}, \quad F_{\text{scale}} = \sigma_2 \mathbf{u} \left(\frac{\mu_0 \mathbf{m}}{4\pi r^3} \right)^2.$$

The distance is taken as $r = 7.7 \cdot 10^{-3}$ m from centre of the permanent magnet to the liquid metal. The coordinate s is the circumferential distance on the pipe surface measured from the line $y=0$. The Lorentz force distribution is clearly correlated with eddy current density distribution and the orientation of the Lorentz force density is mostly opposite to the x -direction.

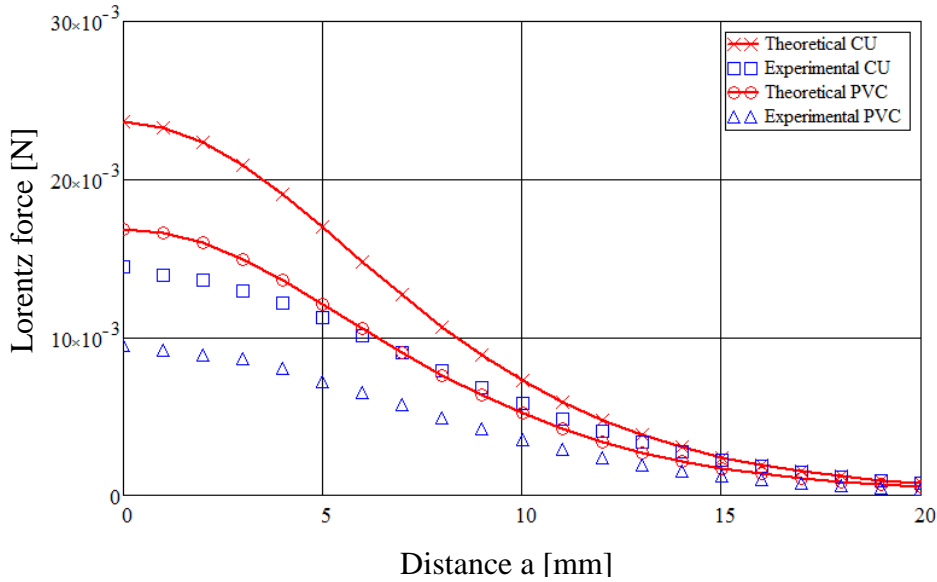


Figure 2: Lorentz force dependence on transverse distance.

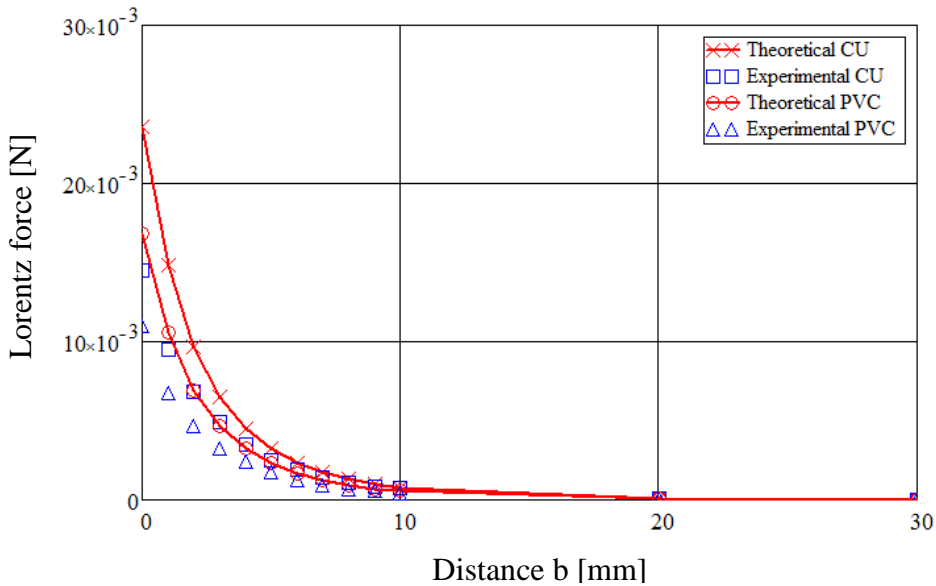


Figure 3: Lorentz force dependence on radial distance.

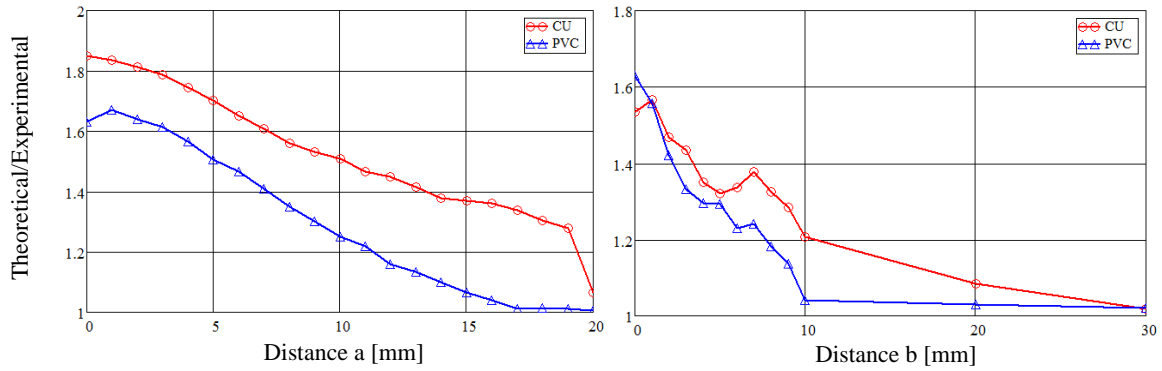


Figure 4: Ratio between theoretical and experimental Lorentz forces.

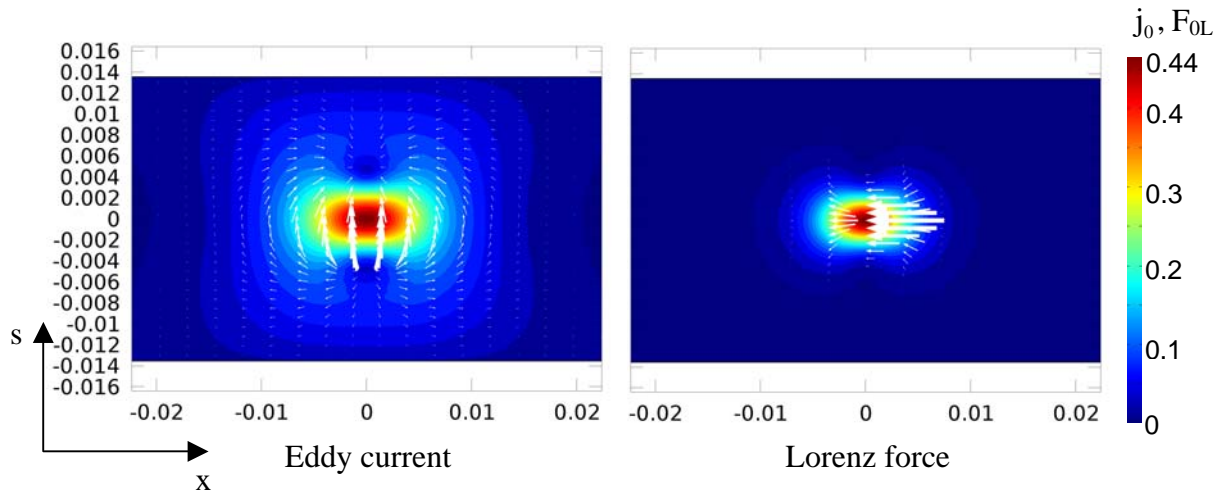


Figure 5: Eddy current and Lorentz force distribution on the inner pipe surface for insulating walls, velocity $u = 1$ m/s, $a=10$ mm and $b=10$ mm.

4. Conclusion We have performed experiments and simulations of a LFV test setup using liquid metal flows in pipes with insulating and conducting walls. The conducting walls are beneficial because they increase the measured force. Further work will focus on velocity variation and a more realistic approximation of the magnetic field.

5. Acknowledgments: The authors acknowledge the financial support by the Deutsche Forschungsgemeinschaft (research training group GRK 1567) and by the Helmholtz Alliance “Liquid Metal Technologies”. The authors also thank M. Zec for sharing his Comsol models for the insulating pipe geometry.

6. References

- [1] Thess A., Votyakov E., Knaepen B., Zikanov O.: Theory of the Lorentz force flowmeter. *New Journal of Physics*, 9 (2007) 299.
- [2] Heinicke C., Tympel S., Pulugundla G., Rahneberg I., Boeck T. and Thess A.: Interaction of a small permanent magnet with a liquid metal duct flow. *Journal of Applied Physics* 112, 124914 (2012).
- [3] Kirpo M., Tympel S., Boeck T., Krasnov D. and Thess A.: Electromagnetic drag on a magnetic dipole near a translating conducting bar *Journal of Applied Physics* 109, 113921 (2011).
- [4] Priede J., Buchenau D., Gerbeth G.: Contactless electromagnetic phase-shift flowmeter for liquid metals. *Meas. Sci. Technol.* 22, 055402 (2011).
- [5] Davidson P.A.: *An introduction to Magnetohydrodynamics*, Cambridge University Press (2001) 432.
- [6] Schade H., Kunz E.: *Strömungslehre*. Walter de Gruyter (2007) 558.